Advances in Applied Mathematics and Mechanics
Adv. Appl. Math. Mech., Vol. **4**, No. 2, pp. 205-222

DOI: 10.4208/aamm.10-m11104
April 2012

Semi-Analytical Solution for Functionally Graded Solid Circular and Annular Plates Resting on Elastic Foundations Subjected to Axisymmetric Transverse Loading

A. Behravan Rad*

Department of Mechanical Engineering, Karaj Branch, Islamic Azad University, Karaj, Iran

Received 26 May 2011; Accepted (in revised version) 30 November 2011

Available online 26 March 2012

Abstract. In this paper, the static analysis of functionally graded (FG) circular plates resting on linear elastic foundation with various edge conditions is carried out by using a semi-analytical approach. The governing differential equations are derived based on the three dimensional theory of elasticity and assuming that the mechanical properties of the material vary exponentially along the thickness direction and Poisson's ratio remains constant. The solution is obtained by employing the state space method (SSM) to express exactly the plate behavior along the graded direction and the one dimensional differential quadrature method (DQM) to approximate the radial variations of the parameters. The effects of different parameters (e.g., material property gradient index, elastic foundation coefficients, the surfaces conditions (hard or soft surface of the plate on foundation), plate geometric parameters and edges condition) on the deformation and stress distributions of the FG circular plates are investigated.

AMS subject classifications: 15A16, 15A18, 65D32, 74B05, 74G15

Key words: Functionally graded circular plate, elastic foundation, differential quadrature method, state-space method.

1 Introduction

Functionally graded materials (FGMs) have gained considerable attention in recent years. FGMs are a new kind of composite materials with wide range of applications. Since their material properties vary as a function with respect to the coordinates, their problems are more complicated than those of the homogeneous materials. FGMs are

*Corresponding author.
Email: behravanrad@gmail.com (A. B. Rad), abehravanrad@aol.com (A. B. Rad)

composite materials that are microscopically inhomogeneous, and their mechanical properties vary continuously in one (or more) direction(s). This is achieved by gradually changing the composition of the constituent materials along one direction, usually in the thickness direction, to obtain smooth variation of material properties and optimum response to the externally applied loading. The static and dynamic analysis of the FGM structural components is important in the design stage. Several researchers can be found in the literature in the field of structural analysis of FGM components using different methods. For example, Chen et al. [1] applied the DQ method to the analysis of geometrically nonlinear vibration of immovably simply supported beams. Reddy et al. [2] investigated axisymmetric bending of an FGM circular plate based on the first-order plate theory and obtained the relationships between the first-order plate theory and the classical thin plate theory. Chen et al. [3] applied the Hadamard and SJT matrices product with differential quadrature (DQ) rule to solution of geometrically nonlinear bending of isotropic and orthotropic rectangular plates. Yang and Shen [4] dealt with the dynamic response of initially stressed functionally graded rectangular thin plates subjected to partially distribute impulsive lateral loads. Ma and Wang [5] studied the axisymmetric bending of an FGM circular plate with the third-order plate theory. Vel and Batra [6] presented a three-dimensional exact solution for free and forced vibrations of simply supported functionally graded rectangular plates. Chen [7] investigated the nonlinear vibration of functionally graded plates with arbitrary initial stresses, effects of the amplitude of vibration, initial conditions and volume fraction on nonlinear vibration were studied. Serge [8] considered the problems of free vibrations, buckling, and static deflections of functionally graded plates whose material properties vary through the thickness. Park and Kim [9] analyzed the thermal post buckling and vibration of the functionally graded plates considering nonlinear temperature-dependent material properties. Nie and Zhong [10] investigated the bending of two-directional FG circular and annular plates based on the three-dimensional theory of elasticity using the state- space method combined with the DQM. Three-dimensional free and forced vibration analysis of functionally graded circular plates with material properties that vary continuously in the thickness direction and various boundary conditions was presented by Nie and Zhong [11]. Li et al. [12] presented the elasticity solutions for a transversely isotropic FGM circular plate subject to an axisymmetric transverse load in terms of the polynomials of even order. Free and forced vibration analysis of functionally graded annular sectorial plates with simply supported radial edges and arbitrary circular edges was carried out by Nie and Zhong [13]. Huang et al. [14] presented an exact solution for FG rectangular thick plates resting on elastic foundations, based on the three-dimensional theory of elasticity, using infinite double series of trigonometric functions combined with the state- space method. Wang et al. [15] applied the direct displacement method to investigate the free axisymmetric vibration of the transversely isotropic circular plates. Malekzadeh [16] used the DQ method to analysis the free vibration of thick FG rectangular plates supported by two-parameter elastic foundations. Hosseini-Hashemi et al. [17] investigated buckling and free vibration behaviors of radially functionally

graded circular and annular sector thin plates subjected to uniform in-plane compressive loads resting on the Pasternak elastic foundation by using the DQ method. Nie and Zhong [18] studied free vibration behavior of two-directional FG circular and annular plates, by using state-space-DQ method. Alibeigloo [19] presented a three-dimensional exact solution for static analysis of simply supported functionally graded material (FGM) rectangular plates imbedded in piezoelectric layers, resting on elastic foundation and subjected to transverse loading. Malekzadeh et al. [20] studied the free vibration analysis of FGMs thick annular plates based on the 3D elasticity theory by using the DQM.

In a survey of literature, the author has found no work on static analysis of functionally graded circular plates resting on elastic foundation. Therefore, this paper deals with static behavior of FGMs circular plates subject to axisymmetric transverse load resting on elastic foundations. The material properties are assumed to be graded in the thickness direction according to an exponential distribution. The formulations are based on the three-dimensional theory of elasticity. A semi-analytical method, which makes use of the state space method and the one-dimensional differential quadrature method, is employed in the static analysis.

2 The governing equations

Fig. 1 illustrates an annular plate constructed from functionally graded materials with outer/inner radius a, b and thickness h, subjected to an axisymmetric transverse load (uniform pressure) resting on a linear two parameter elastic foundation. A cylindrical coordinate system (r,θ,z) whose origin o located at the center of bottom plane of the plate is employed to describe the displacement field. The plate is assumed to be isotropic and heterogeneous at any point of the volume, with a constant Poisson's ratio ν and elastic coefficients that vary exponentially along the transverse direction of the plate according to the following law

$$c_{ij}(z) = c_{ij}^{0} \exp\left[\lambda\left(\frac{z}{h}\right)\right]. \tag{2.1}$$

Moreover, distribution of the material properties, applied loads, and boundary conditions are axisymmetric. Due to the axi-symmetry of the problem, $u_\theta = 0$ and shear

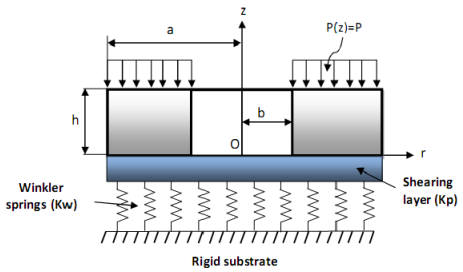

Figure 1: Geometry of FGMs annular plate resting on linear two parameter elastic foundation.

stress components $\tau_{\theta z}=0$, $\tau_{r\theta}=0$, also the derivatives of all parameters with respect to the coordinate θ are identically zero, i.e., $\partial/\partial\theta=0$. Therefore, the equations of equilibrium with neglecting the body forces, the strain-displacement relations and the constitutive equations can be writhen as

$$\frac{\partial\sigma_r}{\partial r}+\frac{\partial\tau_{rz}}{\partial z}+\frac{\sigma_r-\sigma_\theta}{r}=0,\qquad \frac{\partial\tau_{rz}}{\partial r}+\frac{\partial\sigma_z}{\partial z}+\frac{\tau_{rz}}{r}=0, \tag{2.2a}$$

$$\varepsilon_r=\frac{\partial u_r}{\partial r},\qquad \varepsilon_\theta=\frac{u_r}{r},\qquad \varepsilon_z=\frac{\partial u_z}{\partial z},\qquad \gamma_{rz}=\frac{\partial u_r}{\partial z}+\frac{\partial u_z}{\partial r}, \tag{2.2b}$$

$$\begin{cases}\sigma_r=c_{11}(z)\varepsilon_r+c_{12}(z)\varepsilon_\theta+c_{13}(z)\varepsilon_\theta, & \sigma_z=c_{13}(z)\varepsilon_\theta+c_{23}(z)\varepsilon_\theta+c_{33}(z)\varepsilon_z,\\ \sigma_\theta=c_{12}(z)\varepsilon_r+c_{11}(z)\varepsilon_\theta+c_{13}(z)\varepsilon_\theta, & \tau_{rz}=c_{44}(z)\gamma_{rz}.\end{cases} \tag{2.2c}$$

According to Eqs. (2.1)-(2.2), the governing differential equations at bottom surface of the plate can be obtained in terms of displacement components as:

$$\frac{\partial^2u_r}{\partial z^2}=-\frac{c_{11}^0}{c_{44}^0}\Big(\frac{\partial^2u_r}{\partial r^2}+\frac{1}{r}\frac{\partial u_r}{\partial r}-\frac{u_r}{r^2}\Big)-\frac{\lambda}{h}\frac{\partial u_z}{\partial r}-\frac{\lambda}{h}\frac{\partial u_r}{\partial z}-\frac{\partial}{\partial r}\frac{\partial u_z}{\partial z}-\frac{c_{13}^0}{c_{44}^0}\frac{\partial}{\partial r}\frac{\partial u_z}{\partial z}, \tag{2.3a}$$

$$\frac{\partial^2u_z}{\partial z^2}=-\frac{\lambda}{h}\frac{c_{13}^0}{c_{33}^0}\Big(\frac{\partial u_r}{\partial r}+\frac{u_r}{r}\Big)-\frac{c_{44}^0}{c_{33}^0}\Big(\frac{\partial^2u_z}{\partial r^2}+\frac{1}{r}\frac{\partial u_z}{\partial r}\Big)-\frac{c_{13}^0+c_{44}^0}{c_{33}^0}\Big(\frac{\partial}{\partial r}\frac{\partial u_r}{\partial z}+\frac{1}{r}\frac{\partial u_r}{\partial z}\Big)-\frac{\lambda}{h}\frac{\partial u_z}{\partial z}. \tag{2.3b}$$

3 Solutions of the differential equations

In order to solve Eq. (2.3), the semi-analytical approach is used. This method combines the state space method (SSM) to provide an analytical solution along the material gradient direction (z-direction) to express the through-thickness behavior of the plate and the one dimensional differential quadrature method (DQM) to approximate the radial direction effects of the plate. By using this method a linear eigenvalue system in terms of the displacements is established and by solving the resulted eigenvalue system, the static response of the plate is obtained.

3.1 The state space method

By defining the elements of state vector as

$$I=\Big\{u_r\ \ u_z\ \ \frac{\partial u_r}{\partial z}\ \ \frac{\partial u_z}{\partial z}\Big\}^T,$$

the state space notation of Eq. (2.3) can be written as

$$\frac{\partial}{\partial z}\{I\}=\begin{bmatrix}D_1\\ D_2\end{bmatrix}\{I\}, \tag{3.1}$$

where the elements of matrixes D_1, D_2 are given by,

$$D_1=\begin{bmatrix}0&0&1&0\\0&0&0&1\end{bmatrix},\qquad D_2=\begin{bmatrix}d_{11}&d_{12}&d_{13}&d_{14}\\d_{21}&d_{22}&d_{23}&d_{24}\end{bmatrix},$$

with

$$d_{11}=-\frac{c_{11}^0}{c_{44}^0}\Big(\frac{\partial^2}{\partial r^2}+\frac{1}{r}\frac{\partial}{\partial r}-\frac{1}{r^2}\Big), \qquad d_{12}=-\frac{\lambda}{h}\frac{\partial}{\partial r},$$
$$d_{13}=-\frac{\lambda}{h}, \qquad d_{14}=-\frac{\partial}{\partial r}-\frac{c_{13}^0}{c_{44}^0}\frac{\partial}{\partial r},$$
$$d_{21}=-\frac{\lambda}{h}\frac{c_{13}^0}{c_{33}^0}\Big(\frac{\partial}{\partial r}+\frac{1}{r}\Big), \qquad d_{22}=-\frac{c_{44}^0}{c_{33}^0}\Big(\frac{\partial^2}{\partial r^2}+\frac{1}{r}\frac{\partial}{\partial r}\Big),$$
$$d_{23}=-\frac{c_{13}^0+c_{44}^0}{c_{33}^0}\Big(\frac{\partial}{\partial r}+\frac{1}{r}\Big), \qquad d_{24}=-\frac{\lambda}{h}.$$

To normalize the elements of matrix D_2 the following non-dimensional parameters are considered

$$Z=\frac{z}{h}, \qquad R=\frac{r}{a}, \qquad U_R=\frac{u_r}{h}, \qquad U_Z=\frac{u_z}{h}, \qquad c_{ij}^{-0}=\frac{c_{ij}^0}{c_{33}^0}. \tag{3.2}$$

By implement these non-dimensional parameters in Eq. (3.1), the state space notation can be written as

$$\frac{\partial}{\partial Z}\{I\}=\begin{bmatrix} D_1 \\ D_2(R) \end{bmatrix}\{I\}, \tag{3.3}$$

where

$$I=\Big\{U_R \;\; U_Z \;\; \frac{\partial U_R}{\partial Z} \;\; \frac{\partial U_Z}{\partial Z}\Big\}^T,$$

and the elements of $D_2(R)$ are functions of the variable R.

In order to get the solution to Eq. (3.3), the elements of matrix $D_2(R)$ must be converted to constant values with applying the DQM approximation.

3.2 DQM procedure and its application

According to the existing literature [21,22], the principle of DQ rule is stated as follow: for a continuous function $\Phi(r)$ defined in an interval $r\in[0,1]$, its nth order derivative with respect to argument r at an arbitrary given point r_i can be approximated by a linear sum of the weighted function values of $\Phi(r)$ in the whole domain. This procedure can be expressed mathematically as

$$\frac{\partial^{(n)}\Phi(r_i)}{\partial r^n}=\sum_{j=1}^{n}A_{ij}^{(n)}\Phi(r_j), \qquad i=1,2,\cdots,N \quad \text{and} \quad n=1,\cdots,N-1, \tag{3.4}$$

where $A_{ij}^{(n)}$ are the weighted coefficients determined by the coordinates of the sample points r_i.

Explicit expressions of the first and second derivatives of the weighted coefficients matrices and also criterions to adopt non-uniformly spaced grid points are presented in Appendix A.

The partial derivatives of the unknown displacements U_R, U_Z with respect to R in the right-hand side of Eq. (3.3) after applying the DQ rule at an arbitrary point R_i can be expressed as:

$$\frac{\partial U_R}{\partial R}\Big|_{R=R_i} = \sum_{j=1}^{N} A_{ij} U_{Rj}, \quad \frac{\partial U_Z}{\partial R}\Big|_{R=R_i} = \sum_{j=1}^{N} A_{ij} U_{Zj}, \quad \frac{\partial^2 U_R}{\partial R^2}\Big|_{R=R_i} = \sum_{j=1}^{N} B_{ij} U_{Rj}, \tag{3.5a}$$

$$\frac{\partial^2 U_Z}{\partial R^2}\Big|_{R=R_i} = \sum_{j=1}^{N} B_{ij} U_{Zj}, \quad \frac{\partial^2 U_R}{\partial R \partial Z}\Big|_{R=R_i} = \sum_{j=1}^{N} A_{ij} \frac{\partial U_{Rj}}{\partial Z}, \quad \frac{\partial^2 U_Z}{\partial R \partial Z}\Big|_{R=R_i} = \sum_{j=1}^{N} A_{ij} \frac{\partial U_{Zj}}{\partial Z}, \tag{3.5b}$$

where U_{Rj}, U_{Zj}, $\partial U_{Rj}/\partial Z$, $\partial U_{Zj}/\partial Z$ are the state variables values at the discrete point R_j.

By substituting Eq. (3.5) in to (3.3), the state space notation at discrete points is obtained as

$$\frac{\partial}{\partial Z}\{I_i\} = \begin{bmatrix} D_{1i} \\ D_2(R_i) \end{bmatrix} \{I_i\}, \qquad i = 1, \cdots, N, \tag{3.6}$$

where elements of the matrix $D_2(R_i)$ are constants. The elements of matrixes, D_{1i}, $D_2(R_i)$ are given in Appendix B.

According to the rules of matrix operation, the general solution to Eq. (3.6) is:

$$I_i(Z) = e^{ZM_i} I_i(0). \tag{3.7}$$

Eq. (3.7) establishes the transfer relations from the state vector on the bottom surface to that at an arbitrary plane Z of the plate by the exponential matrix of e^{ZM_i}. Setting $Z = 1$ in Eq. (3.7) gives

$$I_i(1) = e^{M_i} I_i(0), \tag{3.8}$$

where e^{M_i} is the global transfer matrix and $I_i(1)$, $I_i(0)$ are the values of the state variables at the upper and lower planes of the plate, respectively.

4 Boundary conditions

The following boundary conditions are considered in this study.

(i) For a solid circular plate $(b = 0)$, the edge boundary conditions are

- Clamped edge (c):

$$u_r = 0, \quad \frac{\partial u_z}{\partial r} = 0 \quad \text{at} \quad r = 0, \tag{4.1a}$$

$$u_r = 0, \quad u_z = 0 \quad \text{at} \quad r = a. \tag{4.1b}$$

- Simply-supported edge (s):

$$u_r = 0, \quad \frac{\partial u_z}{\partial r} = 0 \quad \text{at} \quad r = 0, \tag{4.2a}$$

$$\sigma_r = 0, \quad u_z = 0 \quad \text{at} \quad r = a. \tag{4.2b}$$

(ii) For an annular plate with the inner radius b and outer radius a, the edges conditions are

- Clamped- Clamped in the inner and outer edges $(c-c)$:

$$u_r = 0, \quad u_z = 0 \quad \text{at} \quad r = b, \tag{4.3a}$$

$$u_r = 0, \quad u_z = 0 \quad \text{at} \quad r = a. \tag{4.3b}$$

- Simply-supported-Clamped in the inner and outer edges $(s-c)$:

$$\sigma_r = 0, \quad u_z = 0 \quad \text{at} \quad r = b, \tag{4.4a}$$

$$u_r = 0, \quad u_z = 0 \quad \text{at} \quad r = a. \tag{4.4b}$$

- Free-Clamped in the inner and outer edges $(f-c)$:

$$\sigma_r = 0, \quad \tau_{rz} = 0 \quad \text{at} \quad r = b, \tag{4.5a}$$

$$u_r = 0, \quad u_z = 0 \quad \text{at} \quad r = a. \tag{4.5b}$$

Since the lower surface of the plate supported by a two parameter elastic foundation, the interaction between the plate and foundation is treated as boundary condition. The reaction-deflection relation at the bottom surface of the plate rested on Winkler-Pasternak elastic foundation in an axisymmetric problem can be expressed as

$$\sigma_{z0} = k_w u_{z0} - k_p \Big(\frac{\partial^2 u_{z0}}{\partial r^2} + \frac{1}{r} \frac{\partial u_{z0}}{\partial r} \Big), \tag{4.6}$$

where σ_{z0} is the density of reaction force on the bottom surface of the plate, and u_{z0} is the deflection of that surface. Therefore, the boundary conditions at the bottom and top surfaces of the solid circular and annular plates are

$$\tau_{rz} = 0, \quad \sigma_z = \sigma_{z0} \quad \text{at} \quad z = 0, \tag{4.7a}$$

$$\tau_{rz} = 0, \quad \sigma_z = -P \quad \text{at} \quad z = h. \tag{4.7b}$$

The discretized forms of the edge and regularity conditions for a solid circular plate disscused in Eqs. (4.1)-(4.2) can be expressed as follows:

- Clamped edge (c):

$$U_{RN} = 0, \quad U_{ZN} = 0 \quad \text{at} \quad R = 1. \tag{4.8}$$

- Simply-supported edge (s):

$$\sigma_{RN} = 0, \quad U_{ZN} = 0 \quad \text{at} \quad R = 1. \tag{4.9}$$

- Regularity conditions in the center of the plate:

$$U_{R1}=0, \quad U_{Z1}=-\sum_{j=2}^{N}\frac{A_{1j}}{A_{11}}U_{Zj} \quad \text{at} \quad R=0. \tag{4.10}$$

The discretized forms of the edge conditions for an annular plate expressed in Eqs. (4.3)-(4.5) can be presented as follows:

- Clamped-Clamped in the inner and outer edges $(c-c)$:

$$U_{R1}=0, \quad U_{Z1}=0 \quad \text{at} \quad R=\frac{b}{a}, \tag{4.11a}$$

$$U_{RN}=0, \quad U_{ZN}=0 \quad \text{at} \quad R=1. \tag{4.11b}$$

- Simply supported-Clamped in the inner and outer edges $(s-c)$:

$$\sigma_{R1}=0, \quad U_{Z1}=0 \quad \text{at} \quad R=\frac{b}{a}, \tag{4.12a}$$

$$U_{RN}=0, \quad U_{ZN}=0 \quad \text{at} \quad R=1. \tag{4.12b}$$

- Free-Clamped in the inner and outer edges $(f-c)$:

$$\sigma_{R1}=0, \quad \tau_{RZ1}=0 \quad \text{at} \quad R=\frac{b}{a}, \tag{4.13a}$$

$$U_{RN}=0, \quad U_{ZN}=0 \quad \text{at} \quad R=1. \tag{4.13b}$$

The discretized forms of the boundary conditions at the lower and upper surfaces of the plate, Eqs. (4.7a) and (4.7b) can be written as:

- At $Z=0$,

$$\frac{\partial U_{Ri}}{\partial Z}+\frac{h}{a}\sum_{j=1}^{N}A_{ij}U_{Zj}=0, \tag{4.14a}$$

$$\frac{\partial U_{Zi}}{\partial Z}+\frac{h}{a}c_{13}^{-0}\Big(\sum_{j=1}^{N}A_{ij}U_{Rj}+\frac{U_{Ri}}{R_i}\Big)=\frac{\sigma_{Z0}(R_i)}{c_{33}^{0}}$$

$$=K_W U_{Zi}-K_p\Big(\sum_{j=1}^{N}B_{ij}U_{Zj}+\frac{1}{R_i}\sum_{j=1}^{N}A_{ij}U_{Zj}\Big), \tag{4.14b}$$

$$K_W=\frac{k_w h}{c_{33}^{0}}, \qquad K_p=\frac{k_p}{c_{33}^{0}}\frac{h}{a^2}, \qquad i=1,2,3,\cdots,N, \tag{4.14c}$$

where K_W and K_p are the non dimensional elastic coefficients of the foundation.

- At $Z=1$,

$$\frac{\partial U_{Ri}}{\partial Z}+\frac{h}{a}\sum_{j=1}^{N}A_{ij}U_{Zj}=0, \tag{4.15a}$$

$$\frac{\partial U_{Zi}}{\partial Z}+\frac{h}{a}c_{13}^{-0}\Big(\sum_{j=1}^{N}A_{ij}U_{Rj}+\frac{U_{Ri}}{R_i}\Big)=-\frac{P}{c_{33}^{0}e^{\lambda}}, \qquad i=1,2,3,\cdots,N. \tag{4.15b}$$

By substituting the edge conditions appeared in Eqs. (4.8)-(4.13) and the corresponding boundary conditions presented in Eqs. (4.14), (4.15) in to Eq. (3.6), the following algebraic equations for bending analysis can be obtained

$$GT = Q, \tag{4.16}$$

where G is a $4(N-2) \times 4(N-2)$ matrix, Q is a traction force vector and T is:

$$T = \left[\; U_{Ri}(0) \;\; U_{Zi}(0) \;\; U_{Ri}(1) \;\; U_{Zi}(1) \; \right]^T, \qquad i = 2, 3, \cdots N-1.$$

By solving Eq. (4.16), all state parameters at $Z = 0$, $Z = 1$ are obtained. We can use Eqs. (3.7) and (2.2c) to calculate the displacements and the stresses through the thickness of the FGMs circular plates.

5 Numerical results

In order to extract the numerical results, Aluminum $E_{A1} = 70$GPa and Alumina $E_{cr} = 380$GPa are considered as the metal and ceramic constituents of the FGMs plate. The material properties of the FGM constituents are taken from [9]. The numerical results are derived for a clamped solid circular plate with the geometry $(a = 1.0\text{m}, h = 0.04a)$, and clamped-clamped annular plate with $(a = 1.0\text{m}, b = 0.1\text{m}, h = 0.04a)$ resting on linear elastic foundations. The material properties are assumed to have exponential distributions in the thickness of the plate shown in Eq. (2.1). To achieve the numerical results non-equally spaced discretization points (Appendix B) are considered and the number of discrete points in the radial direction is nine. The plate material data and the boundary conditions on the lower and the upper surfaces of the plate are

$$E_0 = 70\text{GPa}, \quad E_h = 380\text{GPa}, \quad \nu = 0.3, \tag{5.1a}$$

$$\tau_{rz} = 0, \quad \sigma_z = \sigma_{z0} \qquad \text{at } z = 0, \tag{5.1b}$$

$$\tau_{rz} = 0, \quad \sigma_z = -1\text{GPa} \quad \text{at } z = h. \tag{5.1c}$$

The effects of the elastic foundation coefficients, material property graded index, the thickness to radius ratio, the surfaces conditions and the edges support type on static behavior of the FG circular plate are intensively discussed in the following text. The numerical results are derived for the first time and shown in Figs. 4-9.

Since analytical and numerical solutions are not available in literature or the static response of FGMs circular plate resting on elastic foundations, convergence analysis of the present method is a necessity. Therefore, the convergence of the present method is investigated for the following two cases, by solving the small bending deflection of the clamped supported thick circular FGM plate $(h/a = 0.2)$ under a uniformly distributed transverse pressure p.

1. Resting on elastic foundations with coefficients $K_W = K_P = 1$.
2. In the absence of elastic foundations.

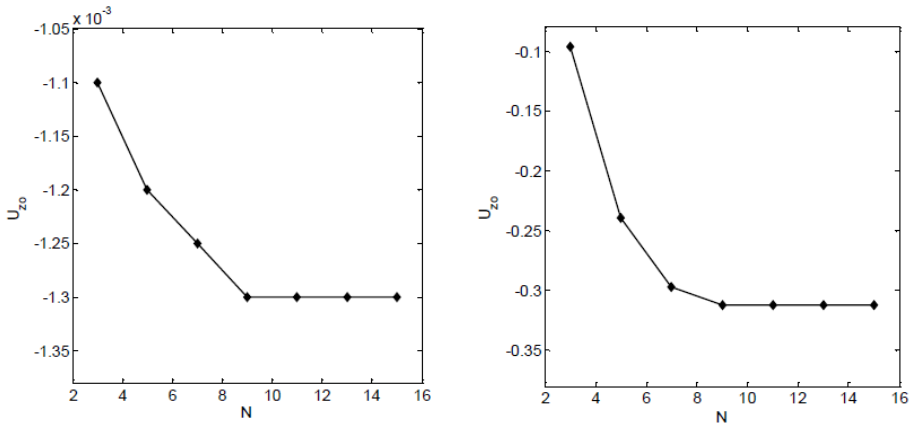

(a) (b)

Figure 2: Convergence of non-dimensional deflection of the plate at $R = 0.5$: (a) on elastic foundations, (b) in the absence of elastic foundations.

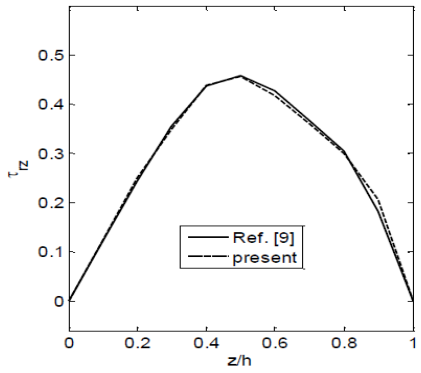

Figure 3: Comparison of the present results with the results found in the literature for a solid FG circular plate in the absence of elastic foundations.

The non-dimensional transverse deflection U_{Z0} vs. number of discrete points N for the above mentioned plate with the data expressed in Eq. (5.1) and $\lambda = 1$ at the mid-point of radius is plotted in Fig. 2. It can be seen from Fig. 2 that the non-dimensional deflection of the plate approaches to a specific value with an increase of the discrete points. This confirms that the convergence of this method is excellent.

For the foregoing reason, for validation, firstly numerical results are derived for a solid circular plate with clamped edge in the absence of elastic foundations and compared with the results of [9]. To achieve the numerical results, structural parameters of the plate are chosen as $(a = 1.0\text{m}, h = 0.1\text{m}, E_0 = 380\text{GPa}, \nu = 0.3, \lambda = 1)$, and the boundary conditions on the top and the bottom surfaces of the plate are considered similar to Eq. (5.1) which are the same as those given in [9]. The curves of extracted data from [9] and present solution are plotted in Fig. 3. From this figure, it can be found that the present results are in good agreement with the available results in [9].

The effects of material property graded index on static behavior of the solid

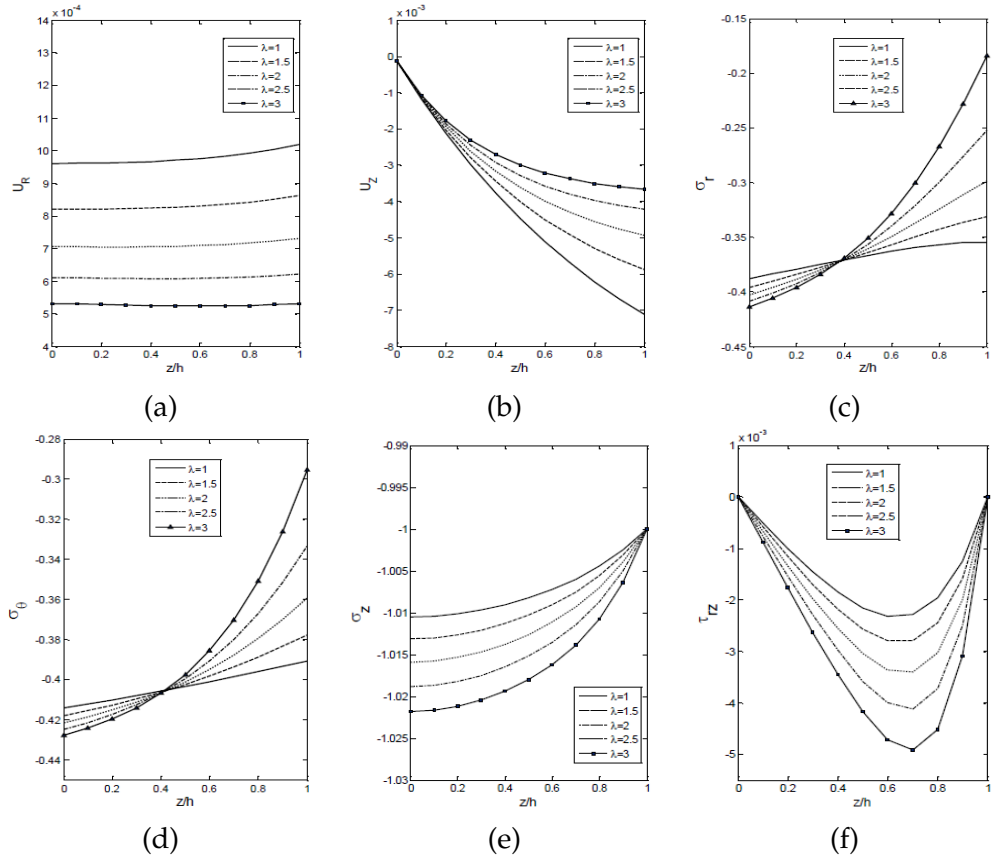

Figure 4: Effect of the material property graded index on variation of displacements and stress components versus z/h at a location $(R = 0.5)$ for a solid circular plate resting on elastic foundation $(K_W = K_P = 1)$ with $h = 0.04a$: (a) radial displacement component U_R, (b) transverse displacement component U_Z, (c) radial stress component σ_r(GPa), (d) tangential stress component σ_θ(GPa), (e) transverse normal stress component σ_z(GPa), (f) transverse shear stress component τ_{rz}(GPa).

clamped plate on linear elastic foundations are plotted in Fig. 4. It is seen from Fig. 4 that U_R and U_Z through-thickness of the plate decrease as λ increase. The value of in-plane stresses increase gradually along the thickness of the plate when z/h is less than 0.4 and then decrease as λ increase. The transverse normal stress σ_z at lower surface of the plate increases with increasing λ and it gradually changes along plate thickness and converges to external load value at upper surface. The pick value of transverse shear stress τ_{rz} increases as λ increases and its values through the thickness of the plate for known λ increases when z/h is less than 0.7 and then decrease. Decrease of displacements through plate thickness indicates that increasing the gradient index will certainly enhance the deformation rigidity of the plate.

The effects of the thickness to radius ratio on static behavior of the plate are plotted in Fig. 5. It is seen from Fig. 5 that the value of U_R, σ_r and σ_θ decrease, and stresses σ_z, τ_{rz} increase gradually as h/a ratio increases. The distribution of the transverse normal and shear stresses through the thickness of the plate converge to the horizontal lines

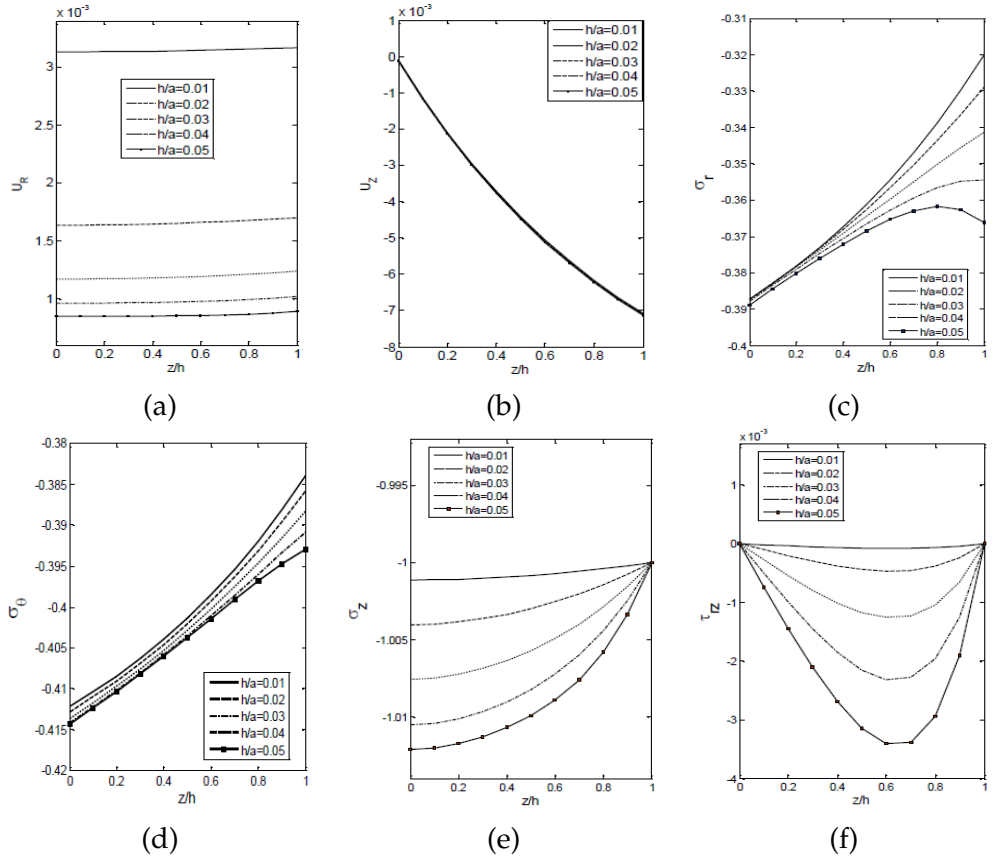

Figure 5: Effect of the thickness to radius ratio on variation of displacements and stress components versus z/h at a location $(R = 0.5)$ for a circular plate resting on elastic foundation $(K_W = K_P = 1)$ with $\lambda = 1$: (a) radial displacement component U_R, (b) transverse displacement component U_Z, (c) radial stress component σ_r(GPa), (d) tangential stress component σ_θ(GPa), (e) transverse normal stress omponent σ_z(GPa), (f) transverse shear stress component τ_{rz}(GPa).

with decreasing the thickness of the plate.

The effect of the inner to outer radius ratios on static behavior of the clamped-clamped annular plate $K_W = K_P = 0.1$ and $\lambda = \ln(E_h/E_0)$ is presented in Fig. 6. It can be found from Fig. 6, that, the displacements at bottom surface and through-thickness of the plate decrease as b/a ratio increases. The values of in plane stresses σ_r and σ_θ decrease in bottom surface of the plate with increasing b/a ratio and along plate thickness σ_r increases when z/h less than 0.6 and then decreases, and σ_θ increase with increasing the b/a ratio. The value of transverse normal stress in bottom surface of the plate decreases with increasing b/a ratio and it values through plate thickness changes gradually and converges to the external load value at top plane for all b/a ratios. The pick value of transverse shear stress τ_{rz} increases as b/a ratio increase.

In the next stage the effects of foundation coefficients (Winkler-Pasternak), together with changing the surfaces position (hard or soft surface) of the plate attached to the foundation are studied, therefore two cases are considered. Case 1: the metal

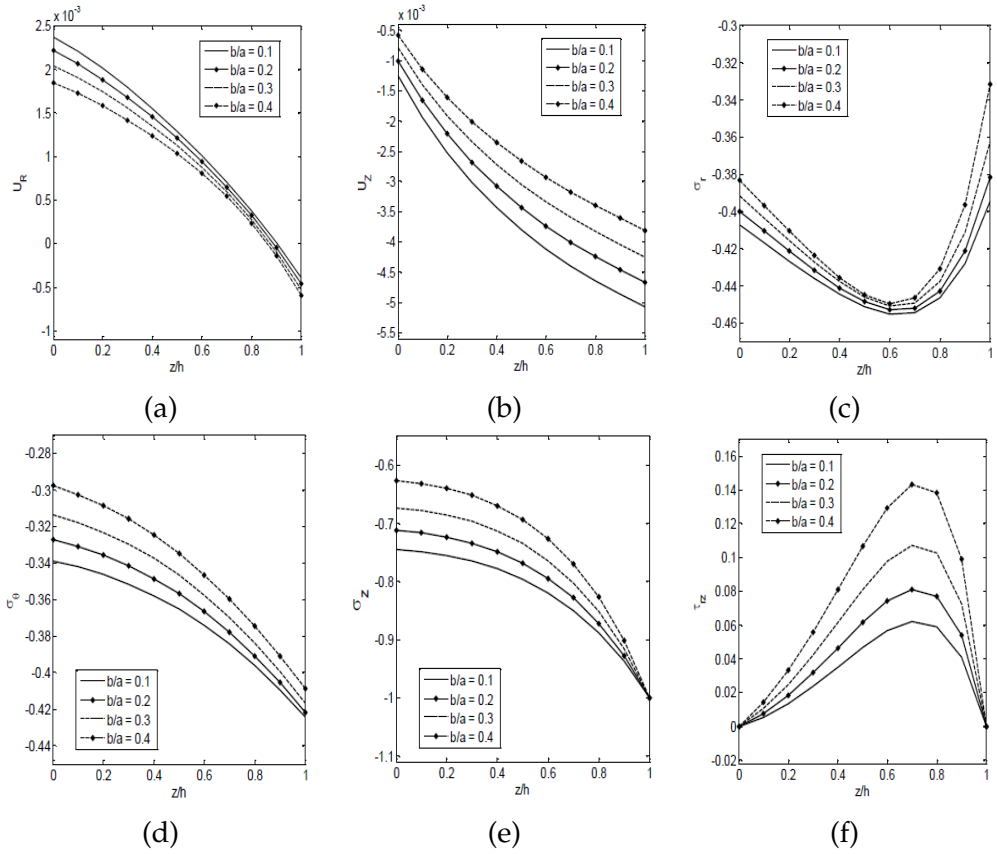

Figure 6: Effect of radius ratio on variation of displacements and stress components versus z/h at a location $(R = 0.97)$ for an annular clamped-clamped plate resting on elastic foundation $(K_W = K_P = 0.1)$, $\lambda = \ln(E_h/E_0)$, $h = 0.04a$ (metal rich plane on the foundation): (a) radial displacement component U_R, (b) transverse displacement component U_Z, (c) radial stress component σ_r(GPa), (d) tangential stress component σ_θ(GPa), (e) transverse normal stress component σ_z(GPa), (f) transverse shear stress component τ_{rz}(GPa).

rich plane attached to the elastic foundation and elastic modulii at the lower and upper surfaces of the plate are $E_0 = 70$GPa, $E_h = 380$GPa, Case 2: the ceramic rich plane attached to the elastic foundation and Young's modulii at the bottom and top surfaces of the plate are $E_0 = 380$GPa, $E_h = 70$GPa.

The effects of foundation stiffness on physical quantities for the Case 1 are plotted in Fig. 7. It can be found from Fig. 7, that U_R, U_Z decrease with increasing K_W, K_P through the thickness direction of the circular FG plate. The value of stress σ_r decreases at bottom surface as K_W, K_P increases and its magnitude for smaller foundation coefficients increase when z/h is less than 0.7 and then decreases, for bigger coefficients gradually increase through the thickness of the plate. The value of stress σ_θ increases through the thickness of the plate as foundation stiffnesses increase. The value of stress σ_z increases, τ_{rz} decreases through the thickness of the plate with increasing the foundation coefficients.

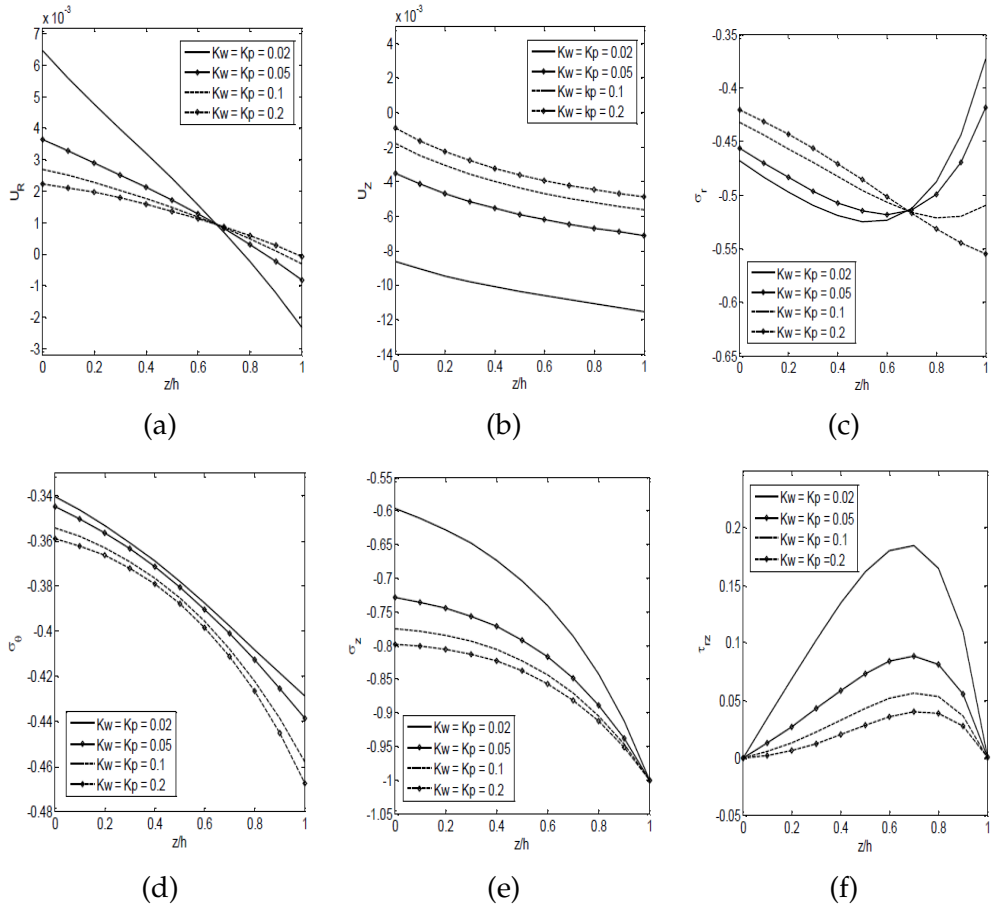

Figure 7: Effect of the elastic foundation coefficients on variation of displacements and stress components versus z/h at a location $(R = 0.96)$ for a circular plate resting on elastic foundation with $\lambda = \ln(E_h/E_0)$, $h = 0.04a$ (metal rich plane on the foundation): (a) radial displacement component U_R, (b) transverse displacement component U_Z, (c) radial stress component σ_r(GPa), (d) tangential stress component σ_θ(GPa), (e) transverse normal stress component σ_z(GPa), (f) transverse shear stress component τ_{rz}(GPa).

The influences of foundation stiffness on physical quantities for the Case 2 are plotted in Fig. 8. It is observed from Fig. 8, that U_R, U_Z, σ_r, τ_{rz} decrease and stresses σ_θ, σ_z increase as increase K_W, K_P. Comparison of the results in Figs. 5 and 6 show that the magnitude or variation schemes of the displacements and stresses relative to the physical location in the plate of Case 1 and Case 2 are considerably different. The curvatures of U_Z, σ_r and σ_θ through thickness in the Case 2 are different that of in Case 1.

The effect of supports on variation of transverse normal and shear stresses through thickness for the plate is plotted in Fig. 9. According to the figure, it can be seen that the maximum variation of τ_{rz} through thickness of the plate at a desired location occurs for free-clamped annular plate.

Distribution of transverse normal stress through thickness of the plate at a desired

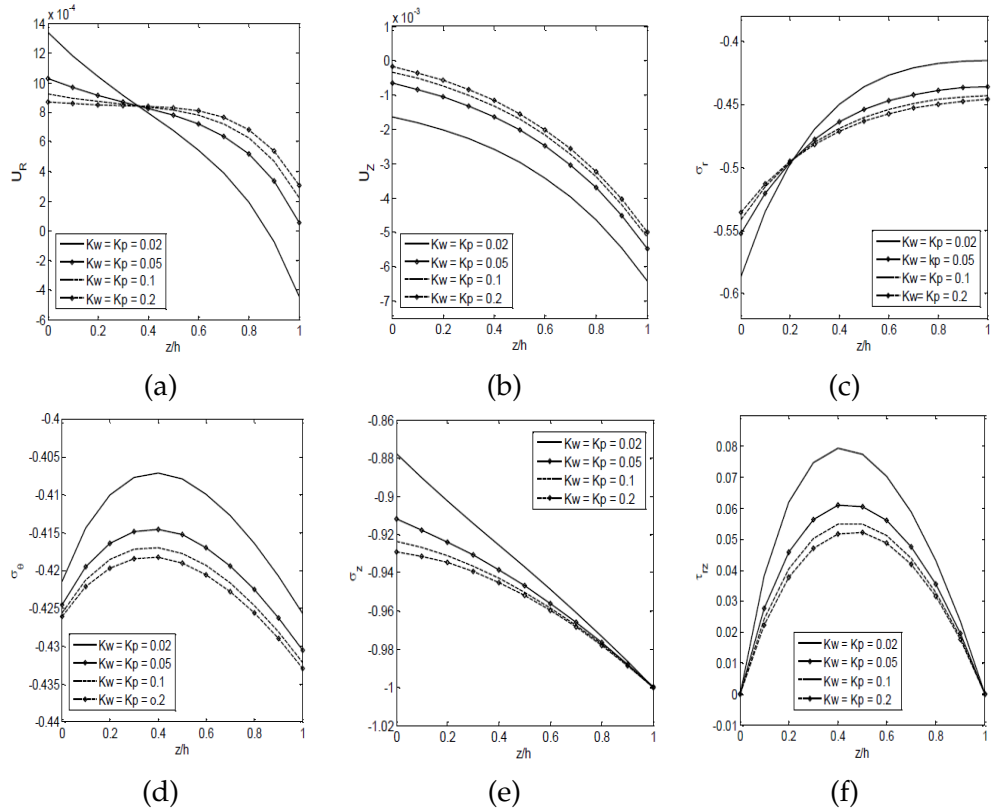

Figure 8: Effect of the elastic foundation coefficients on variation of displacements and stress components versus z/h at a location $(R = 0.96)$ for a solid circular plate resting on elastic foundation with $\lambda = \ln(E_h/E_0)$, $h = 0.04a$ (ceramic rich plane on the foundation): (a) radial displacement component U_R, (b) transverse displacement component U_Z, (c) radial stress component σ_r(GPa), (d) tangential stress component σ_θ(GPa), (e) transverse normal stress component σ_z(GPa), (f) transverse shear stress component τ_{rz}(GPa).

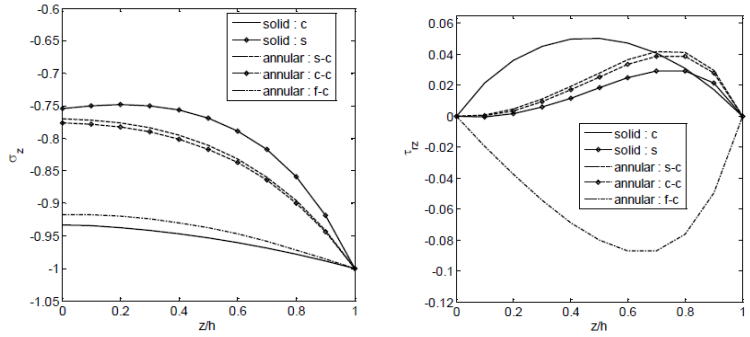

Figure 9: Effect of edge supports on variation of transverse stress components versus z/h at a location $(R = 0.96)$ for a solid circular and annular plates, resting on elastic foundation with $K_W = K_P = 1$, $\lambda = \ln(E_h/E_0)$, $h = 0.04a$ (metal rich plane on the foundation): (a) transverse normal stress component σ_z(GPa), (b) transverse shear stress component τ_{rz}(GPa).

location lies between clamped and simply supported edges plate. Variation scheme of transverse shear stress through thickness for the plate with free-clamped and clamped support is different with variation scheme of this quantity to other supports.

6 Conclusions

Axisymmetric static analysis of functionally graded circular plates resting on Winkler-Pasternak elastic foundation with various boundary conditions are investigated in this paper using semi-analytical approach (SSM-DQM). By using this method some results are carried out, with the most important conclusions that:

- The effects of foundation stiffness on mechanical responses of the plate are considerably different, and that, for a given FGM circular plate, the mechanical behavior of the plate with the softer (metal rich) surface supported by elastic foundation differ significantly from that of the plate with the harder (ceramic rich) surface subjected to the same foundation.
- The neutral surface of the FGM is not at the mid-surface but depends on the through-thickness variation of Young's moduli.
- The distribution of the transverse normal and shear stresses through the thickness of the plate converge to the horizontal lines with decreasing the thickness of the plate, which is the characteristic of the thin plate.
- The effect of elastic foundation coefficients on the through-thickness stresses is much more than that of the in-plane stresses.

Appendix A

The elements of weighting coefficients of the first-order derivative matrix A can be obtained from the following algebraic formulation [22],

$$A_{ik} = \frac{\prod_{j=1,\ j\neq i}^{N} (r_i - r_j)}{(r_i - r_k)M(r_k)}, \qquad i \neq k,\ \ i,k = 1,\cdots,N,$$

$$A_{ii} = -\sum_{j=1,\ j=i}^{N} A_{ij}, \qquad i = k,\ \ i,k = 1,\cdots,N.$$

The weighting coefficients of the second-order derivative can be obtained from the following recurrence relation [22]

$$B_{ik} = 2\Big[A_{ii}A_{ik} - \frac{A_{ik}}{r_i - r_k}\Big], \qquad i \neq k,\ \ i,k = 1,\cdots,N,$$

$$B_{ii} = -\sum_{j=1,\ j=i}^{N} B_{ij}, \qquad i = k,\ \ i,k = 1,\cdots,N.$$

The following criterions are used for nodes discretization

1. Richard-Shu criterion for solid circular plates

$$r_i = \frac{1}{2}\Big[1-\cos\Big(\frac{(i-1)\pi}{N-1}\Big)\Big], \qquad i=1,\cdots,N.$$

2. Chebyshev criterion for annular plates

$$r_i = b+\frac{1}{2}\Big[1-\cos\Big(\frac{(i-1)\pi}{N-1}\Big)\Big](a-b), \qquad i=1,\cdots,N.$$

Appendix B

For matrices

$$D_{1i} = \begin{bmatrix} 0 & 0 & [\delta_{ij}]_{N\times N} & 0 \\ 0 & 0 & 0 & [\delta_{ij}]_{N\times N} \end{bmatrix}_{2N\times 4N},$$

we have

$$\delta_{ij}=0 (i\neq j), \qquad \delta_{ii}=1,$$

$$D_2(R_i) = \begin{bmatrix} [d_{ij}^{11}]_{N\times N} & [d_{ij}^{12}]_{N\times N} & [d_{ij}^{13}]_{N\times N} & [d_{ij}^{14}]_{N\times N} \\ [d_{ij}^{21}]_{N\times N} & [d_{ij}^{22}]_{N\times N} & [d_{ij}^{23}]_{N\times N} & [d_{ij}^{24}]_{N\times N} \end{bmatrix}_{2N\times 4N},$$

$$d_{ij}^{11} = -\frac{c_{11}^0}{c_{44}^0}\Big(\frac{h}{a}\Big)^2\Big(\sum_{j=1}^{N} B_{ij}+\frac{1}{R_i}\sum_{j=1}^{N} A_{ij}-\frac{1}{R_i^2}\Big), \qquad d_{ij}^{12} = -\frac{\lambda h}{a}\sum_{j=1}^{N} A_{ij},$$

$$d_{ij}^{13} = 0, \qquad d_{ij}^{14} = -\frac{h}{a}\Big(1+\frac{c_{13}^0}{c_{44}^0}\Big)\sum_{j=1}^{N} A_{ij},$$

$$d_{ij}^{21} = -\frac{\lambda h}{a}\frac{c_{13}^0}{c_{33}^0}\Big(\sum_{j=1}^{N} A_{ij}+\frac{1}{R_i}\Big), \qquad d_{ij}^{22} = -\frac{c_{44}^0}{c_{33}^0}\Big(\frac{h}{a}\Big)^2\Big(\sum_{j=1}^{N} B_{ij}+\frac{1}{R_i}\sum_{j=1}^{N} A_{ij}\Big),$$

$$d_{ij}^{23} = -\frac{c_{13}^0+c_{44}^0}{c_{33}^0}\frac{h}{a}\Big(\sum_{j=1}^{N} A_{ij}-\frac{1}{R_i}\Big), \qquad d_{ii}^{24} = -\lambda, \qquad d_{ij}^{24} = 0.$$

References

[1] W. CHEN, S. LIANG AND T. ZHONG, *On the DQ analysis of geometrically nonlinear vibration of immovably simply supported beams*, J. Sound. Vib., 206(5) (1997), pp. 745–748.

[2] J. N. REDDY, C. M. WANG AND S. KITIPORNCHAI, *Axisymmetric bending of functionally graded circular and annular plates*, Euro. J. Mech. Solids., 18 (2) (1999), pp. 185–199.

[3] W. CHEN, C. SHU AND W. HE, *The DQ solution of geometrically nonlinear bending of orthotropic rectangular plates by using Hadamard and SJT product*, Comput. Struct., 74(1) (2000), pp. 65–74.

[4] J. YANG AND H. S. SHEN, *Dynamic response of initially stressed functionally graded rectangular thin plates*, Comp. Struct., 54 (2001), pp. 497–508.

[5] L. S. MA AND T. J. WANG, *Relationships between axisymmetric bending and buckling solutions of FGM circular plates based on third-order plate theory and classical plate theory*, Int. J. Solids. Struct., 41(1) (2004), pp. 85–101.
[6] S. S. VEL AND R. C. BATRA, *Three-dimensional exact solution for the vibration of functionally graded rectangular plates*, J. Sound. Vib., 272 (2004), pp. 703–730.
[7] C. S. CHEN, *Nonlinear vibration of a shear deformable functionally graded plate*, Comp. Struct., 68 (2005), pp. 295–302.
[8] A. SERGE, *Free vibration, buckling, and static deflections of functionally graded plates*, Comp. Sci. Tech., 66 (2006), pp. 2383–2394.
[9] J. S. PARK AND J. H. KIM, *Thermal post buckling and vibration analyses of functionally graded plates*, J. Sound. Vib., 289 (2006), pp. 77–93.
[10] G. J. NIE AND Z. ZHONG, *Axisymmetric bending of two-directional functionally graded circular and annular plates*, Acta. Mech. Solid. Sin., 20(4) (2007), pp. 289–295.
[11] G. J. NIE AND Z. ZHONG, *Semi-analytical solution for three-dimensional vibration of functionally graded circular plates*, Comput. Meth. Appl. Mech. Eng., 196 (2007), pp. 4901–4910.
[12] X. Y. LI, H. J. DING AND W. Q. CHEN, *Elasticity solutions for a transversely isotropic functionally graded circular plate subject to an axisymmetric transverse load qr^k*, Int. J. Solids. Struct., 45(1) (2008), pp. 191–210.
[13] G. J. NIE AND Z. ZHONG, *Vibration analysis of functionally graded sectorial plates with simply supported radial edges*, Comp. Struct., 84 (2008), pp. 167–176.
[14] Z. Y. HUANG, C. F. LU AND W. Q. CHEN, *Benchmark solution for functionally graded thick plates resting on Winkler-Pasternak elastic foundations*, Comp. Struct., 85 (2008), pp. 95–104.
[15] Y. WANG, R. Q. XU AND H. J. DING, *Free axisymmetric vibration of FGM plates*, Appl. Math. Mech., 30(9) (2009), pp. 1077–1082.
[16] P. MALEKZADEH, *Three-dimensional free vibration analysis of thick functionally graded plates on elastic foundations*, Comp. Struct., 89 (2009), pp. 367–373.
[17] H. HOSSEINI, H. AKHAVAN, D. T. ROKNI, N. H. DAEMI AND A. ALIBEIGLOO, *Differential quadrature analysis of functionally graded circular and annular sector plates on elastic foundation*, Mater. Design., 31(4) (2010), pp. 1871–1880.
[18] G. J. NIE AND Z. ZHONG, *Dynamic analysis of multi-directional functionally graded annular plates*, Appl. Math. Model., 34(3) (2010), pp. 608–616.
[19] A. ALIBEIGLOO, *Three-dimensional exact solution for functionally graded rectangular plate with integrated surface piezoelectric layers resting on elastic foundation*, Mech. Adv. Mater. Struct., 17(3) (2010), pp. 1–14.
[20] P. MALEKZADEH, S. A. SHAHPARI AND H. R. ZIAEE, *Three-dimensional free vibration of thick functionally graded annular plates in thermal environment*, J. Sound. Vib., 329 (2010), pp. 425–442.
[21] C. SHU, Differential Quadrature and Its Application in Engineering, Springer Publication, New York, 2000.
[22] Z. ZONG AND Y. ZHANG, Advanced Differential Quadrature Methods, CRC Press, New York, 2009.